JOURNAL OF SOLID STATE CHEMISTRY 115, 295–298 (1995)

LETTER TO THE EDITOR

An Unexpected Double Valence Change for Cerium during the Thermal Decomposition of $CeK_2(NO_3)_6$

N. Guillou, J. P. Auffredic, and D. Louër

Laboratoire de Cristallochimie, CSIM (URA CNRS 1495), Université de Rennes, I, Avenue du Général Leclerc, 35042 Rennes Cedex, France

Communicated by J. M. Honig, December 20, 1994

Two successive changes of the oxidation state of cerium were observed when a mixed cerium potassium nitrate, $CeK_2(NO_3)_6$, was heated. The formation of a cerium (III) phase, $Ce_2K_3(NO_3)_9$, together with CeO_2 and KNO_3, during the first stage of decomposition was clearly demonstrated by modeling the X-ray powder diffraction pattern. This cerium (III) compound decomposes into CeO_2 in a second stage. The processes of reduction of cerium (IV), induced by thermal decomposition, and of subsequent oxidation of cerium (III) are discussed.

Compounds of Ce (III) and Ce (IV) with low thermal stability, e.g., oxalates and nitrates, can be used as precursors of nanoscale particles of CeO_2. Recently, a new oxide nitrate of cerium (IV) was reported, giving nanocrystalline oxide at 200°C from its thermal decomposition (1). In the course of the study of cerium (IV) precursors containing nitrate groups, we have also reported the crystal structure determination of two polymorphic phases of $CeK_2(NO_3)_6$ (2, 3). Here we describe the noteworthy successive oxidation state changes of cerium observed in the course of the thermal decomposition of this mixed cerium (IV) potassium nitrate, using the modern developments of powder diffraction with conventional X-ray sources.

Figure 1 shows the three-dimensional representation of the successive powder diffraction patterns of the monoclinic variety of $CeK_2(NO_3)_6$ carried out in vacuum, in the temperature range 20–400°C, obtained by means of a thermodiffractometric system based on a semifocusing arrangement described elsewhere (4). It can be seen that the precursor transforms into pure nanocrystalline CeO_2 through three stages. Similar behavior is obtained under a nitrogen atmosphere and also from the hexagonal variety of $CeK_2(NO_3)_6$. The successive stages of the thermal decomposition are summarized in Table 1. The first step corresponds to the simultaneous formation of CeO_2 and β-KNO_3, together with a third phase identified as $Ce_2K_3(NO_3)_9$ from inspection of its powder diffraction pattern (2, 5). Surprisingly, this phase contains cerium with a +3 oxidation state. In order to demonstrate the unexpected formation of this compound of Ce (III) during the thermal decomposition of the Ce (IV) precursor, the diffraction pattern of the three-component mixture has been modeled by the Rietveld method. The sample was obtained from $CeK_2(NO_3)_6$ heated at 160°C in a nitrogen atmosphere and then cooled at room temperature. A precise powder diffraction pattern was obtained at 22°C with a high-resolution powder diffractometer using a monochromatic radiation (6). To prevent a further transformation of the mixture during data collection, the sample was kept under an inert atmosphere.

The crystal structure of $Ce_2K_3(NO_3)_9$ (2, 5) was selected as starting model for the third phase in the Rietveld refinement, together with that of γ-KNO_3 obtained on cooling β-KNO_3. According to previous studies (7, 8), γ-KNO_3 is stable on cooling between about 124 and 100°C, this temperature range being dependent on the thermal treatments. In the present case, it is interesting to note that the γ phase has been stabilized at room temperature. Since the diffraction lines of the nanocrystalline CeO_2 are very broad, they were considered as contributing to the overall background of the diffraction pattern, which was described by a cubic spline function. The Rietveld refinement was carried out with the program FULLPROF (9), based on the program described by Wiles and Young (10). The final calculation involved 38 parameters, including 21 structural parameters for $Ce_2K_3(NO_3)_9$ and 5 for γ-KNO_3. The details of the refinement are given in Table 2. Figure 2 shows the final fit between observed and calculated patterns. It corresponds to satisfactory structure model and profile indicators (Table 2). The final atomic coordinates for the two refined structures have been listed by Guillou (2). They are in good agreement within three standard deviations, on average, with those reported in the literature (2, 5, 8), which is a satisfactory result for such a complicated pattern. The modeling of

0022-4596/95 $6.00

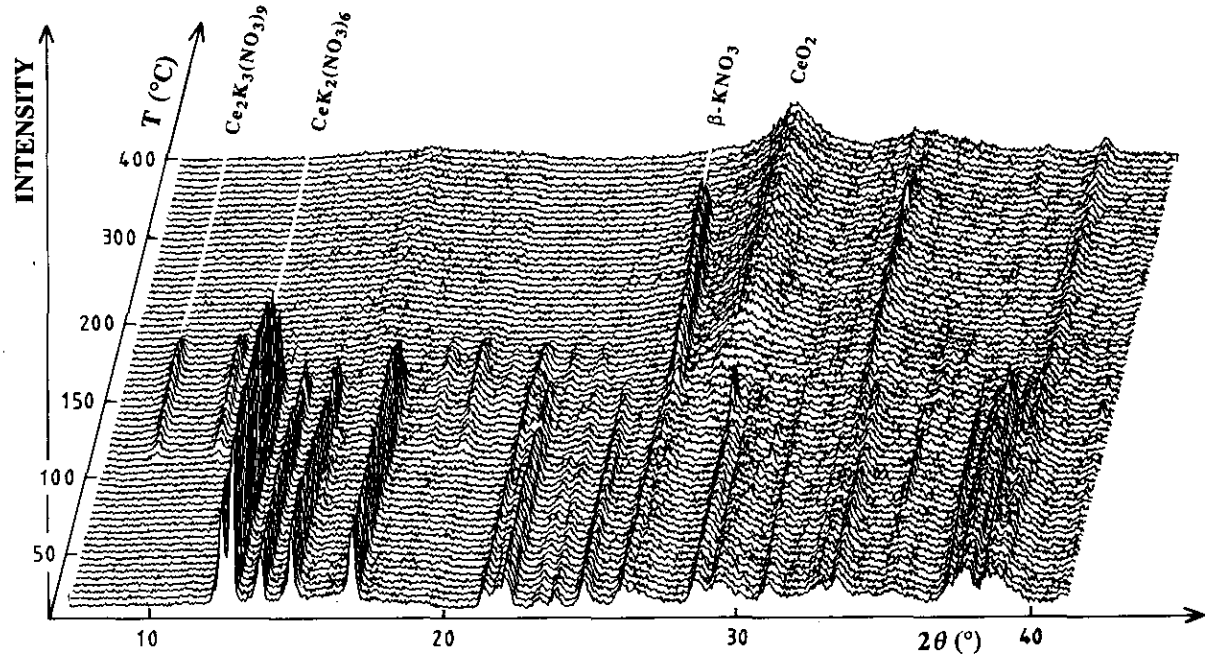

FIG. 1. 3D high-temperature powder diffraction plot (λ = 1.54059 Å) of monoclinic $CeK_2(NO_3)_6$ in vacuum (heating rates: 5°C · hr^{-1} in the range 20–220°C and 10°C · hr^{-1} at higher temperature).

the diffraction pattern of the mixture of the three phases clearly shows the formation of $Ce_2K_3(NO_3)_9$ during the thermal decomposition of $CeK_2(NO_3)_6$. It demonstrates that a redox reaction takes place in the solid state when the precursor is heated. Since cerium (IV) is also found in CeO_2 formed at the same time, only a part of the Ce (IV) atoms of the precursor are reduced into Ce (III). It has been found that the amount of $Ce_2K_3(NO_3)_9$ formed is dependent on the precursor mass, the heating rate, and the environmental atmosphere. By using a precursor mass of 15 mg and a heating rate of 2°C · hr^{-1} and operating under a vacuum of 1.3 Pa, the end of the first decomposition stage is characterized on the TG curve by an inflection point for a weight loss of about 23%. The corresponding amount of KNO_3 produced is thus close to 70%, as calculated from the changes in the integrated intensity of the diffraction line 012 of β-KNO_3. These results show that approximately half the Ce (IV) atoms in $CeK_2(NO_3)_6$ is reduced during the first stage of the decomposition, while the second half remains with a +4 oxidation state in CeO_2.

The second stage of the decomposition process is the transformation of $Ce_2K_3(NO_3)_9$ into CeO_2 and β-KNO_3 (Table I). Therefore, there is again a change in the oxidation state of cerium from III to IV. The last stage corresponds to the melting of β-KNO_3 at 336°C and to the complex decomposition of liquid KNO_3 (11). It can be noted in Table 1 that there is a significant difference between the final temperature of the second stage determined from X-ray diffraction and from the TG curve. This can be explained from the slow release of the gaseous products NO, NO_2, and O_2, which remain adsorbed on the finely divided oxide produced.

Therefore, the phenomenon occurring during the thermal decomposition of $CeK_2(NO_3)_6$ is related to two suc-

TABLE 1
The Successive Stages of the Thermal Decomposition of the Monoclinic Form of $CeK_2(NO_3)_6$

Stage	Transformation	$\Delta m/m_0$ (%) observed	$\Delta m/m_0$ (%) calculated	Temperature range (°C) (X rays)	Temperature range (°C) (TG)
1	$4\ CeK_2(NO_3)_6 \Downarrow Ce_2K_3(NO_3)_9 + 2\ CeO_2 + 5\ \beta\text{-}KNO_3 + x\ NO + (10 - x)\ NO_2 + (3 + x/2)\ O_2$	23	23.54	120–170	115–180
2	$Ce_2K_3(NO_3)_9 \Downarrow 2\ CeO_2 + 3\ \beta\text{-}KNO_3 + x\ NO + (6 - x)NO_2 + (1 + x/2)\ O_2$	13.0	13.04	180–192	180–270
3	Melting and decomposition of β-KNO_3	35.0	34.26	300–336	380–610

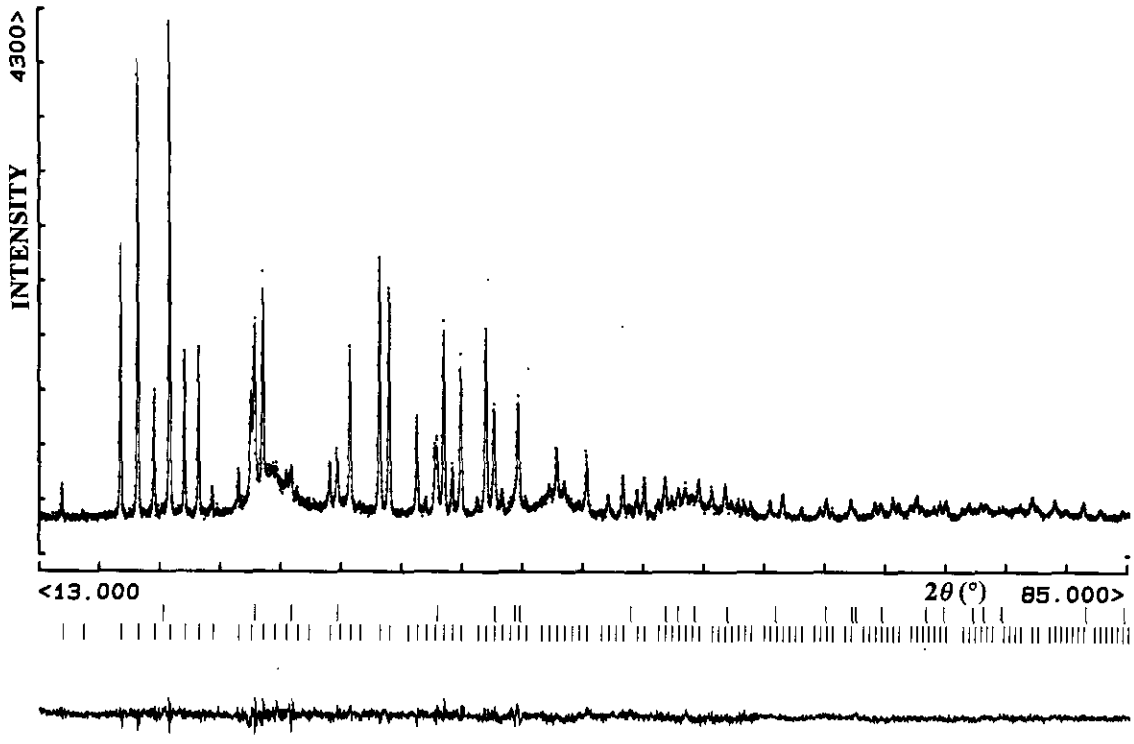

FIG. 2. The final Rietveld plot for the mixture of the three phases $Ce_2K_3(NO_3)_9$, γ-KNO_3, and CeO_2. In the upper portion, the observed data are shown by the dots; the calculated pattern is displayed by the solid line; the lower curve is a plot of the difference, observed minus calculated. The vertical markers below the profile indicate the positions calculated for the Bragg reflections of $Ce_2K_3(NO_3)_9$ (bottom) and of γ-KNO_3 (top).

cessive redox reactions where Ce^{4+} ions are reduced to Ce^{3+}, which in turn undergo a further oxidation into Ce^{4+}. The redox reaction occurring at the first stage is equivalent to

$$2Ce^{4+} + O^{2-} \rightarrow 2Ce^{3+} + 1/2\,O_2,$$

where the O^{2-} anions arise from the breakdown of N–O bonds in nitrate groups. On the other hand, the formation of CeO_2 from the thermal decomposition of $Ce_2K_3(NO_3)_9$, instead of Ce_2O_3, can be explained from the oxygen partial pressure inside the reactor (12).

To conclude, the use of the powerful powder diffraction methods thermodiffractometry and diffraction pattern modeling has clearly demonstrated that a double valence change of cerium occurs during the thermal decomposition of $CeK_2(NO_3)_6$. If disproportionation reactions induced by heating have been described for a few compounds of metals having several oxidation states, e.g., $KMnO_4$ (13), simple redox reactions involving only the reduction or the oxidation of the metallic cation seem less frequent, e.g., the oxidation reaction of Co during the decomposition process of cobalt nitrate (14). To our knowledge, the reduction of cerium (IV) simply induced by thermal decomposition, followed by an oxidation of cerium (III), is the first example in the chemistry of cerium salts of successive simple redox reactions produced during a thermal treatment. It sheds new light on the complex mechanisms of the thermal decomposition of cerium (IV) nitrates and related phases.

TABLE 2
Details of the Rietveld Refinement

	$Ce_2K_3(NO_3)_9$	γ-KNO_3
a (Å)	13.5840(3)	5.4623(3)
c (Å)		9.0163(9)
V (Å^3)	2506.6(2)	232.96(5)
Z	8	3
Wavelength (Å)	1.54059	
2θ range (°)	13–85	
Step scan increment (°2θ)	0.02	
No. of reflections	214	28
No. of structural parameters	21	5
No. of profile parameters	12	
R_B	0.07	0.10
R_{wp}	0.06	

REFERENCES

1. N. Guillou, J. P. Auffrédic, and D. Louër, *J. Solid State Chem.* **112,** 45 (1994).

2. N. Guillou, Thesis. University of Rennes I, July 5, 1994.
3. N. Guillou, M. Louër, J. P. Auffrédic, and D. Louër, *Acta Crystallogr. Sect. C*, in press (1995).
4. J. P. Auffrédic, J. Plévert, and D. Louër, *J. Solid State Chem.* **84,** 58 (1990).
5. N. Guillou, J. P. Auffrédic, and D. Louër, *Acta Crystallogr. Sect. C*, in press (1995).
6. D. Louër and J. I. Langford, *J. Appl. Crystallogr.* **21,** 430 (1988).
7. C. N. R. Rao, B. Prakash, and M. Natarajan, "Crystal Structure Transformations in Organic Nitrites, Nitrates and Carbonates," Pub. NBS-NSRDS-53, p. 1. National Bureau of Standards, Washington, DC, 1975.
8. J. K. Nimmo and B. W. Lucas, *Acta Crystallogr. Sect. B* **32,** 1968 (1976).
9. J. Rodriguez-Carvajal, *in* 'Collected Abstracts of Powder Diffraction Meeting, Toulouse, France, July 1990" (J. Galy, Ed.), p. 127.
10. D. B. Wiles and R. A. Young, *J. Appl. Crystallogr.* **14,** 149 (1981).
11. K. H. Stern, *J. Phys. Chem. Ref. Data* **1,** 3, 747 (1972).
12. D. J. M. Bevan and J. Kordis, *J. Inorg. Nucl. Chem.* **26,** 1509 (1964).
13. V. V. Boldyrev, *J. Phys. Chem. Solids* **30,** 1215 (1969).
14. A. Malecki, A. Malecka, R. Gajerski, B. Prochowska-Klish, and A. Podgorecka, *J. Thermal Anal.* **34,** 203 (1988).